The Pharmacogenomics Journal
https://doi.org/10.1038/s41397-020-0153-6

ARTICLE

Rational design of small molecule RHOA inhibitors for gastric cancer

Jin-Hee Kim[1] · Sungjin Park[2,3] · Seung Mook Lim[4] · Hyo Jin Eom[5] · Curt Balch[6] · Jinhyuk Lee[7,8] · Gi Jin Kim[4] · Jin-Hyun Jeong[1] · Seungyoon Nam[2,3,9,10] · Yon Hui Kim[11]

Received: 30 July 2019 / Revised: 21 January 2020 / Accepted: 23 January 2020

Abstract

Previously, we identified Ras homologous A (RHOA) as a major signaling hub in gastric cancer (GC), the third most common cause of cancer death in the world, prompting us to rationally design an efficacious inhibitor of this oncogenic GTPase. Here, based on that previous work, we extend those computational analyses to further pharmacologically optimize anti-RHOA hydrazide derivatives for greater anti-GC potency. Two of these, JK-136 and JK-139, potently inhibited cell viability and migration/invasion of GC cell lines, and mouse xenografts, diversely expressing RHOA. Moreover, JK-136′s binding affinity for RHOA was >140-fold greater than Rhosin, a nonclinical RHOA inhibitor. Network analysis of JK-136/-139 vs. Rhosin treatments indicated downregulation of the sphingosine-1-phosphate, as an emerging cancer metabolic pathway in cell migration and motility. We assert that identifying and targeting oncogenic signaling hubs, such as RHOA, represents an emerging strategy for the design, characterization, and translation of new antineoplastics, against gastric and other cancers.

Introduction

Gastric cancer (GC) is the fifth most common, and third most lethal, cancer in the world [1]. GC is over three times more prevalent throughout East Asia and South America, compared with other Western nations [2]. Surgery is effective as a first line treatment for early-stage GC, providing a >60% 5-year survival rate [3]. However, early detection is rare, and the overall five-year survival is <20% [3], underscoring the urgent need for improved therapeutics.

It is known that activation of Ras homologous A (RHOA), a small guanine triphosphate-hydrolyzing enzyme (GTPase), triggers a downstream set of complex pathways responsible for gastrulation and angiogenesis [4, 5]. Moreover, RHOA is a mediator of the metastasis-facilitating epithelial-to-mesenchymal transition (EMT) [6, 7]. Analogously, RHOA facilitates the single-tumor cell peritoneal “seeding” that occurs in gastric and other cancers [8, 9].

These authors contributed equally: Jin-Hee Kim, Sungjin Park

Supplementary information The online version of this article (https://doi.org/10.1038/s41397-020-0153-6) contains supplementary material, which is available to authorized users.

✉ Seungyoon Nam
nams@gachon.ac.kr

✉ Yon Hui Kim
yonhuisarahkim@gmail.com

1 College of Pharmacy, Yonsei Institute of Pharmaceutical Sciences, Yonsei University, Incheon 21983, Korea

2 College of Medicine, Gachon University, Incheon 21565, Korea

3 Gachon Institute of Genome Medicine and Science, Gachon University Gil Medical Center, Incheon 21565, Korea

4 Department of Biomedical Science, CHA University, Gyeonggi-do 13486, Korea

5 Research and Development Department, Corestem Inc., Gyeonggi-do 13486, Korea

6 Bioscience Advising, Ypsilanti 48198 MI, USA

7 Genome Editing Research Center, Korea Research Institute of Bioscience and Biotechnology (KRIBB), Daejeon 34141, Korea

8 Department of Bioinformatics, KRIBB School of Bioscience, Korea University of Science and Technology (UST), Daejeon 34113, Korea

9 Department of Life Sciences, Gachon University, Seongnam, Gyeonggi-do 13120, Korea

10 Department of Health Sciences and Technology, GAIHST, Gachon University, Incheon 21999, Korea

11 Department of Biomedical Science, Hanyang Biomedical Research Institute, Hanyang University, Seoul 04763, Korea

Despite initial R0 resection, peritoneal metastases pre-exist in 10–20% of initial diagnoses, and ultimately develop in 60% of advanced GC cases [10].

Previously, one RHOA inhibitor, Rhosin [11], was discovered as strongly antineoplastic against hepatocellular cancer cells [12]; however, Rhosin did not advance beyond animal studies. Previously, we used our subpathway-based computational algorithm, PATHOME [13], to implicate RHOA as a central mediator of gastric tumor progression [13, 14]. Subsequently, we used a systematic approach to identify second-generation, hydrazide derivative RHOA inhibitors, for eventual GC clinical therapy [15]. The *RHOA* mRNA expression in early-stage GC patients was higher in tumor tissue than in its adjacent normal tissues [15]. In GC, RHOA associates with Lauren classification diffuse subtype as well as with poorly differentiated have been recognized [16]. These evidences support clinical significance of RHOA in GC. In terms of biological functions, RHOA activation was involved in actin reorganization, cell motility, and cell migration in GC [15–17]. Also, in GC, RHOA downstream was associated with the WNT pathway, focal adhesion, chemokine signaling and RHOA/Rock pathway [15–17]. Despite no approved RHOA inhibitors by the U.S. Food and Drug Administration (FDA) in GC, clinical efficacy of chemotherapeutic agents in GC was associated RHOA signaling [16]. Thus, RHOA has been considered as a potential biological target in GC [16]. Here, we performed further lead optimization of that inhibitor ("JK-122") [15], for specific treatment of GC, resulting in the identification of two promising small molecule RHOA inhibitors, JK-136 and JK-139. Also, the network analysis of JK-136/-139 treatment, compared with Rhosin, revealed different functional contexts, for numerous GC phenotypes.

Materials and methods

Cell culture

The following human GC cell lines were used within 6 months of resuscitation: AGS (ATCC, Mansfield, VA, USA), SNU-16, SNU-216, SNU-601, SNU-668 (KCLB) and MKN-1 (RIKEN) were cultured in RPMI-1640 (Invitrogen, Carlsbad, CA, USA) and 10% fetal bovine serum (FBS; Hyclone, Logan, UT, USA), at 37 °C and 5% CO_2. Cell line identities were validated by short tandem repeat profiling (ATCC).

Mouse/in vivo experiments

All vertebrate animal experiments were approved by the Korea Preclinical Center Institutional Animal Care and Use Committee (Protocol P175003). Approximately 1×10^7 MKN-45 and SNU-601 cells, grown in log phase, were suspended in 0.2 mL phosphate-buffered saline, and subcutaneously injected into the flanks of severe combined immunodeficient (*scid*) mice (Animal Resource Centre, WA, Australia). For details, please see Supplementary Method S1.

Immunohistochemistry

For mouse xenograft model experiments, immunohistochemical staining was performed on 4-μm tissue sections from paraffin-embedded tissue blocks, using an automated staining instrument, Discovery XT (Ventana Medical Systems, Tuscon, AZ, USA). Please see Supplementary Method S1 for details.

Organic synthesis of hydrazide derivatives

All reactions sensitive to air or moisture were conducted under nitrogen. Reagents were purchased from Sigma-Aldrich and Tokyo Chemical Institute. All anhydrous solvents were distilled over CaH_2, P_2O_5, or Na/benzophenone, prior to the reaction, unless otherwise stated (Fig. 1). For further detailed methods, please see Supplementary Method S1.

Solubility assay

The solubility of compounds was measured using a SPECTRAMAX 190 (Molecular Devices, San Jose, CA, USA). Small volumes (5 μL, 50 mM) of compound solution, dissolved into DMSO, were added to the aqueous buffer solution (pH 7.4). Precipitates were then separated by filtration, and solubility determined by UV absorbance.

Parallel artificial membrane permeability assay (PAMPA)

Please see Supplementary Method S1 [18].

Determination of acid dissociation constants and partition coefficients (pKa and logP)

pK_a and logP values were determined by UV- and pH-metric methods, using a Sirius (East Sussex, UK) T3 instrument, equipped with a pH electrode, UV dip probe, precision micro dispenser, six-way valve for distributing reagents and titrants (0.5 M KOH, 0.5 M HCl, 0.15 M KCl, water-saturated octanol, and MeOH), temperature sensor, and an overhead stirrer. The sample solution volume was 5 μL in 10 mM DMSO, for pKa, and the sample weight for logP assays was 1 mg. A minimum of three replicates, per compound, was performed, at 25 °C. pKa values were

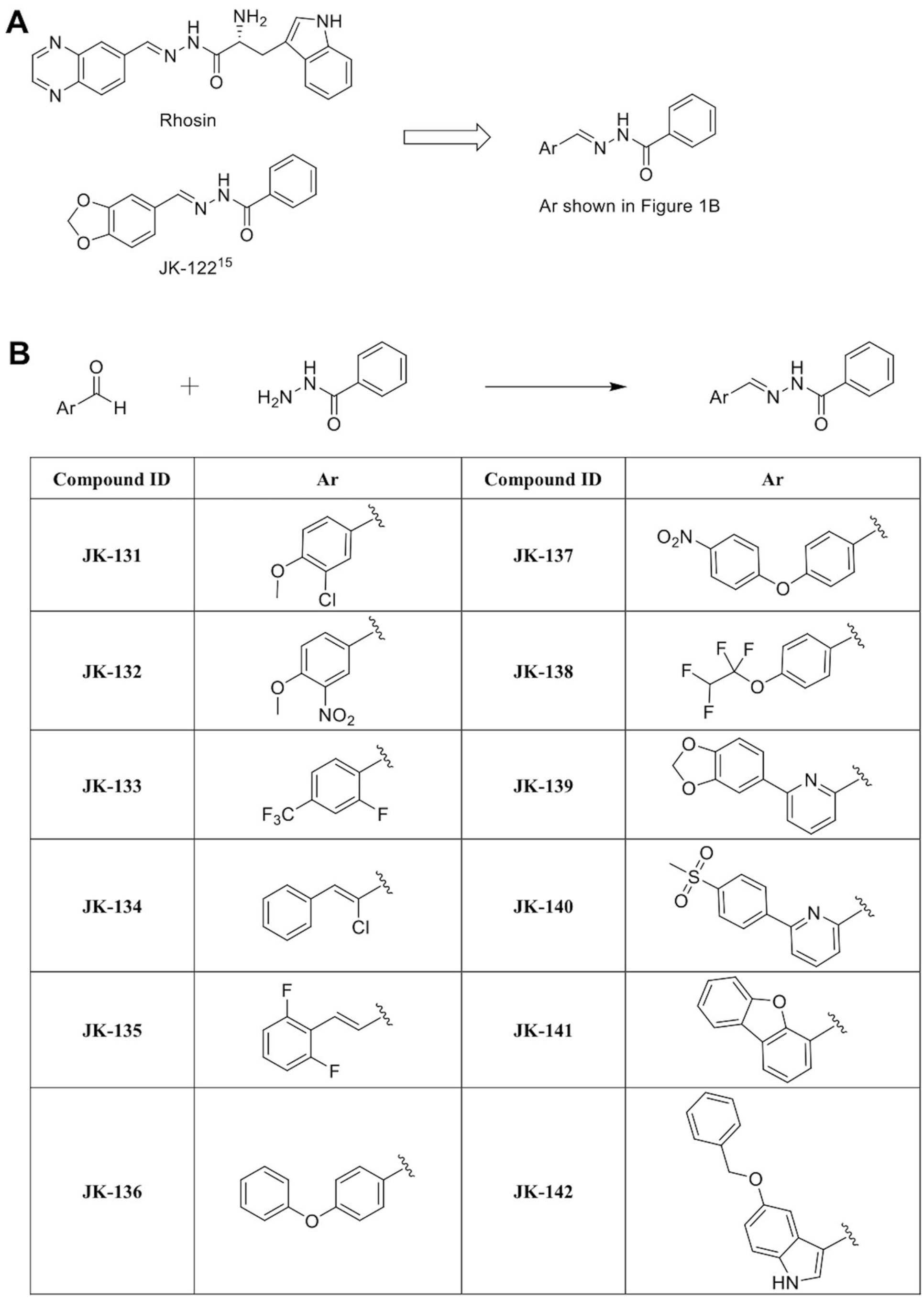

Fig. 1 Novel inhibitors of RHOA. a Rationale for the design of novel RHOA inhibitors. **b** Strategy for synthesizing the desired hydrazide derivatives. Reagents and conditions: MeOH or EtOH, reflux, 0.5–6 h.

determined from 22.57 to 49.60 wt% methanol/water solutions, using Yasuda–Shedlovsky extrapolation [19].

Molecular docking analysis

Docking was performed using Surflex-Dock (Sybyl-X 2.1.1, Tripos Inc, St. Louis, MO, USA), and the software used to construct the structures of compounds JK-131~142, as ligands for RHOA. For the protein, a protocol that generates the binding site of a receptor was used, in conjunction with a ligand-based approach. All other parameters were set to default settings. Energy was minimized by the Powell method, using Gasteiger−Marsili charge and Tripos force field [20]. The crystal structure of RHOA was obtained from the Protein Data Bank (PDB code 4D0N), and all crystal water molecules were removed. Missing hydrogen atoms were added to the structures.

Surface plasmon resonance (SPR)

SPR was used to study RHOA binding to various synthesized small molecules. The Reichert SR7500DC system

(Reichert Technologies, Lancaster, NY, USA) was used, and RHOA (SRP5127, Sigma-Aldrich, Korea) protein was immobilized on CMDH gold chips (Reichert), at 5 μg and a flow rate of 10 μL/min. Rhosin (Millipore, Burlington, MA, USA) and compounds JK-136 and JK-139 were dissolved into DMSO. Immobilized RHOA resulted in 4200 resonance units. Software Scrubber 2.0 [21] (BioLogic Software, Australia) was used to analyze the kinetics of protein-small molecule binding.

Cell viability assays

Please see Supplementary Method S1.

Western blot analysis

Please see Supplementary Method S1.

Migration assay

Please see Supplementary Method S1.

Cell cycle analysis

Please see Supplementary Method S1.

Rho GTPase activity assays

The amounts of active and GTP-bound RHOA, CDC42, and RAC1 were determined using an RHOA, CDC42, and RAC1 G-LISA Activation Assay kits, according to the manufacturer's (Cytoskeleton Inc., Denver, CO, USA) instructions. Briefly, AGS, MKN-1, and SNU-601 GC cells were treated with JK-136 or JK-139 for 48 h. Protein lysates were collected for subsequent analysis by G-LISA, using constitutively active RHOA, CDC42, and RAC1 protein as positive controls. A microplate reader then measured absorbances at 490 nm, to obtain %activities.

Network analysis

JK-136, JK-139, Rhosin, and DMSO control at a concentration of 10 μM were used to treat three GC cell lines (AGS, MKN-1, and SNU-601), performed in triplicate. Total mRNA was then isolated using RNeasy kits (Qiagen), reverse-transcribed, and hybridized to gene expression microarrays (Thermo Fisher Scientific).

To assess functional activity, we used Ingenuity Pathway Analysis® (IPA, Qiagen, Hilden, Germany) [22], resulting in *Z*-scores for pathway activation/inhibition). For network generation following JK-136/-139 treatment, compared with the DMSO control, IPA analyzed gene expression, while IPA Path Explorer tool combined WNT5A and RHOA signaling (two pathways we previously implicated in GC progression) [13–15], into one network. To simplify the network, zero-degree nodes (genes, proteins) were removed.

To identify functional context (i.e., mechanistic) differences between JK-136/-139 and Rhosin, we obtained common significantly ($P < 0.05$ by two-sided t tests) expressed genes between JK-136- and JK-139-treated cells, compared with Rhosin. These analyses identified significantly differentially expressed genes that were then input into IPA by using Fisher's exact tests, resulting in functional context differences.

Results

Rationale and synthesis of a RHOA inhibitor

Figure 1a shows our overall approach for the design of novel RHOA inhibitors, based on JK-122 [15], affecting the phenyl ring, by using a variety of hydrazide spacer lengths, including an alkenyl group (an aliphatic system), a phenyl group (an aromatic system), and a pyridyl group (a heterocyclic system).

To synthesize hydrazides, benzhydrazide was used, whose reaction with numerous aldehydes, in methanol or ethanol at room temperature (or heating), afforded the corresponding final products, JK-131–142 (Fig. 1b).

RHOA inhibitor selection

We assessed IC_{50} values of the final products against three GC cell lines (Fig. 2a and Supplementary Table S1). To evaluate possible cell line dependence on RHOA signaling, cells were selected based on RHOA expression level (high, mid, and low), as in our previous study [15]. Briefly, low-to-high RHOA expression levels were observed in a majority of GC cells, including AGS (low), MKN-1 (medium), and SNU-601 (high); these were then chosen for further experimentation. Only JK-136 and JK-139 exhibited acceptable IC_{50} values (<25.0 μM) (Supplementary Table S1 and Fig. 2a). Cell viability in other cell lines was described in Supplementary Fig. S1.

We next investigated possible mechanisms of GC cell growth inhibition by JK-136 and -139, using flow cytometry, showing that except for a slight JK-136-induced increase of sub-G0 DNA debris in MKN-1, AGS, and SNU-601 cells, no other significant cell cycle changes were observed (Supplementary Fig. S2). However, migration assays showed significant inhibition of wound healing, by both drugs, in all three GC cell lines (Fig. 2b).

Physicochemical properties of the compounds are summarized in Table 1 and Supplementary Table S2, including

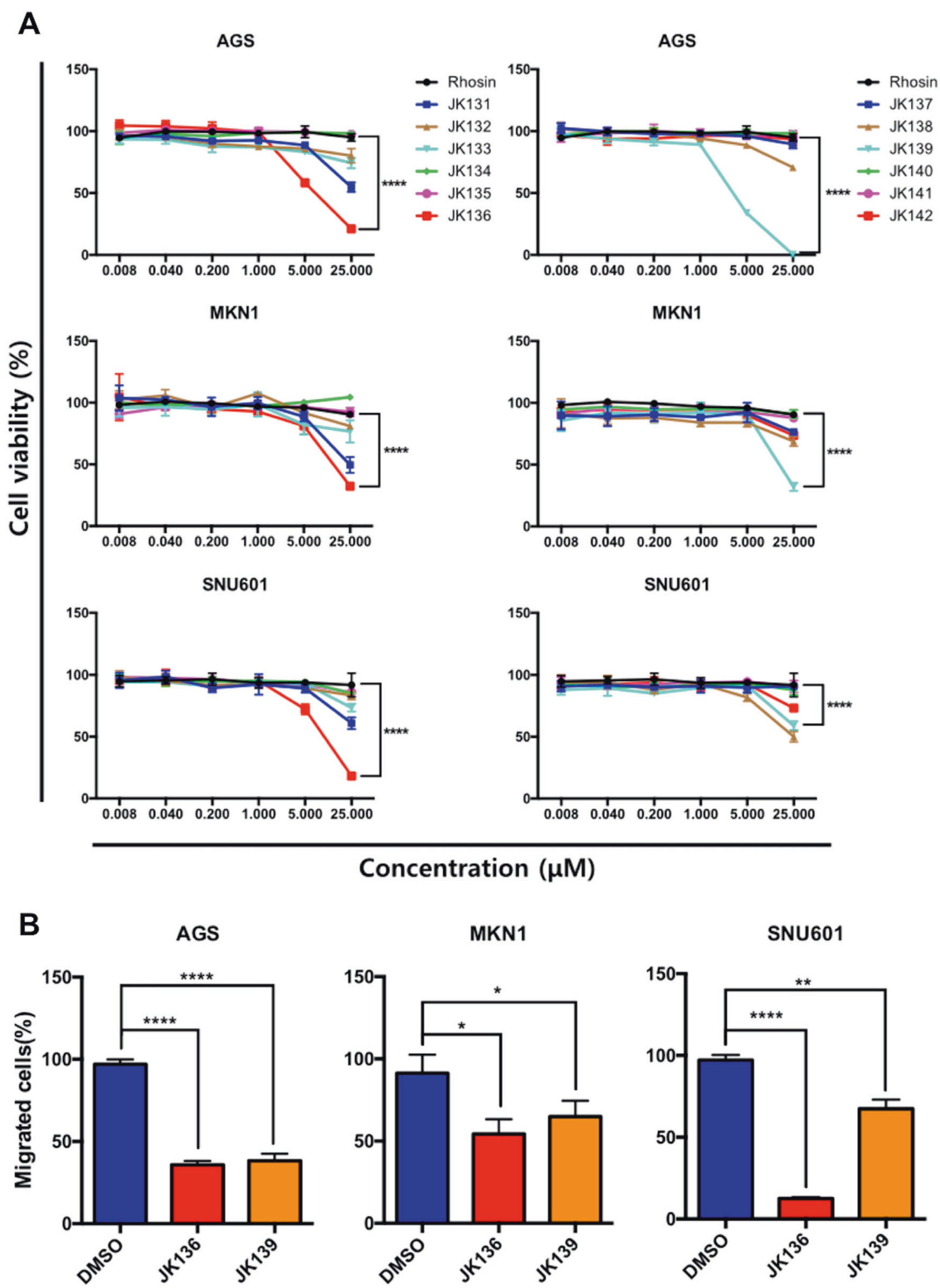

Fig. 2 Small molecule RHOA inhibitors oppose cell growth and migration in GC. a GC cell lines, AGS, MKN-1, and SNU-601 were treated with the 12 small molecule candidates. **b** The migration assay of the three cell lines showed significant inhibition of wound healing by both JK-136 and -139, in three cell lines (*$p < 0.05$, **$p < 0.01$, ****$p < 0.001$).

determinations of solubility and PAMPA, a blood–brain barrier model [18]. The results of the pK_a and logP determination of compounds, JK-136 and JK-139, are depicted in Table 1. LogP, the logarithm of the octanol–water partition coefficient, predicted the compounds' lipophilicities by their relative distributions in the biphasic equilibrium of

Table 1 Determination of acidic dissociation constants and partition coefficients of JK-136 and JK-139.

Compounds	pK_{a1}	pK_{a2}	LogP
JK-136	11.27 ± 0.01	ND	1.28
JK-139	2.99 ± 0.03	10.74 ± 0.02	1.76

ND not detected.

octanol and water, experimentally measured as acid dissociation constants (pK_a).

JK-136 had one acidic pK_a value of 11.27 ± 0.01, while JK-139 a basic pK_a value of 2.99 ± 0.03, and an acidic pK_a of 10.74 ± 0.02 (Table 1). Because JK-139 can either donate or accept a proton, its basic pK_a was lower than its acidic pK_a. pK_a values were measured in aqueous-methanol solution, using the Yasuda–Shedlovsky equation [19] to reveal theoretical pK_as in pure water, showing a logP of 1.28, for JK-136, 1.76, for JK-139, both acceptable lipophilicities for oral absorption.

Molecular docking studies

Based on their efficacy in preliminary in vitro studies, we selected JK-136 and -139 for further characterization and development. Molecular docking analysis of JK-136 and JK-139 binding to the RHOA active site (PDB code 4D0N), used the Surflex-Dock module, implemented in SYBYL-2.1.1 (Tripos, Inc., St. Louis, MO, USA).

Pocket binding of ligands and amino acid residues is displayed in Fig. 3, superimposing JK-136 (purple), JK-139 (green), and Rhosin (orange), represented by the Connolly surface, for possible binding modes (Fig. 3a, b). Interactions of the hydrophobic residues, in the active site pocket of RHOA (brown in Fig. 3a), stabilize the ligand inhibitor. Figure 3c, d shows the predicted hydrogen bonding networks of JK-136 (purple) and JK-139 (green), to key amino acid residues (displayed as stick representations), with carbon atoms in gray, nitrogen atoms in blue, and oxygen atoms in red. The rest of the protein is displayed as red for helixes, yellow for sheets, and green for loops, in ribbon cartoon representation.

The oxygen on the carbonyl group of JK-136 (Fig. 3c) accepts hydrogen bonds from the hydrogens on the amine groups of TYR19 and CYS20, at distances of 2.51 and 2.10 Å, respectively. As shown in Fig. 3d, the oxygen on the piperonyl group of JK-139 interacts with the hydrogen on the amine group of ALA161 through hydrogen bonding, at a distance of 1.82 Å.

Biological evaluation of potential molecules targeting RHOA

We next performed protein (RHOA)-small molecule analysis by SPR, showing that JK-136 had the lowest dissociation constant, K_D, 3.0 ± 0.1 μM (140-fold smaller than Rhosin) of the three drugs (Fig. 4a). Analogously, only JK-136 significantly inhibited RHOA GTPase activity assays showed that only significant RHOA inhibition for three differentially-RHOA-expressing GC cells (Fig. 4b), RAC1 activity was inhibited in only one of the three GC cells (Fig. 4c), and no inhibitor affected CDC42 activity (Fig. 4d), thus validating the SPR results.

Thus, based on binding, and cell growth and enzymatic inhibition, JK-136 and -139 were the most promising, specific RHOA inhibitors.

Network analysis of compound-treated cell lines

In our previous report [13], WNT signaling was elevated in late-stage GC patients. Here, we assessed WNT signaling following JK-136 and JK-139 treatment, using a network analysis tool, IPA [22]. Those results showed that the two compounds downregulated (Z-score < 0) WNT and colorectal cancer metastasis signaling (Fig. 5a; Supplementary Table S3) between JK-136/-139 treatments and DMSO (as control) treatments in three GC cell lines (AGS, MKN-1, and SNU-601). Considering RHOA as a cancer metastasis mediator [15], IPA indicated that WNT components connect to RHOA signaling. Consequently, we then used IPA to merge RHOA and WNT signaling into a single molecular network, including gene expression (Supplementary Fig. S3A, B) for JK-136 and -139 treatments in comparison with DMSO (as controls) treatments in the three GC cell lines. The resultant network also showed RHOA signaling annotated to IPA function terms (processes) such as myofiber contraction, cytoskeleton reorganization, and actin polymerization/nucleation. These processes facilitate cell motility, concurring with our in vitro GC cell migration experiments for JK-136 and -139. Moreover, gene expression comparisons between the two compounds showed similar fold-changes, compared with DMSO treatment. However, differential expression of WAVE complex actin cytoskeletal regulation genes (*WASF1*, *WASF2*) [23], and the hepatocyte nuclear factor-α (HNF4α) gene, was also observed (Fig. 5b, c; Supplementary Fig. S3A, B). Of note, JK-136 downregulated both *HNF4A* and *WNT5A* components of our previously reported GC signaling axis [14]. Also, IPA showed dysregulation of apoptosis- and cell cycle-related pathways (Supplementary Fig. S3A, B).

Next, we inspected functional context (i.e., mechanistic) differences between JK-136/-139 and Rhosin, in GC, showing common genes between JK-136/-139- and Rhosin-treated cells, and significant functional IPA terms (Supplementary Table S4). One such term was sphingosine-1-phosphate (S1P) signaling [24], with two genes, *ASAH2B* (N-acylsphingosine amidohydrolase 2B, i.e., ASAH) and

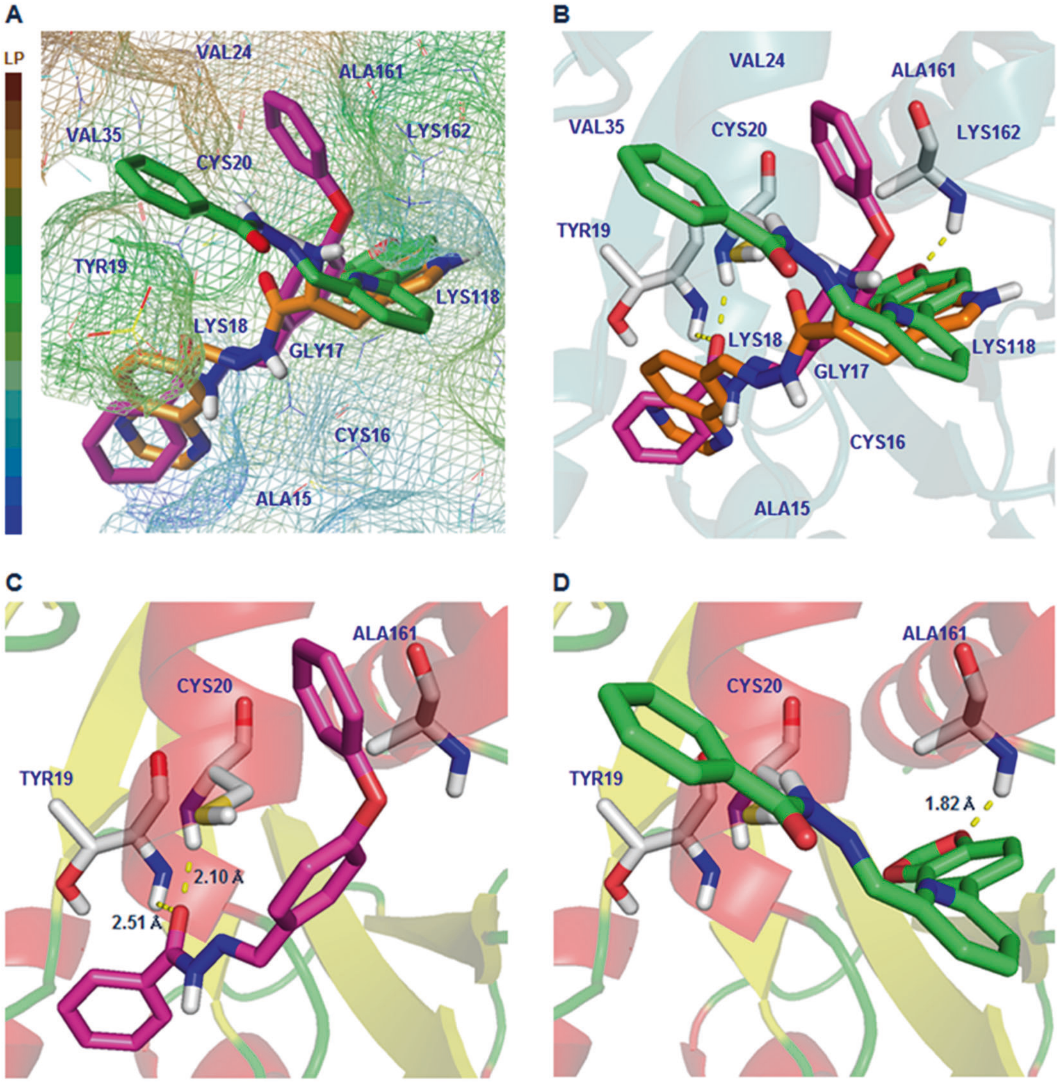

Fig. 3 Binding pockets and potential binding interactions of the investigated molecules in the active site of RHOA (PDB code 4D0N). Hydrogen bonds are denoted as yellow dotted lines. **a** The predicted binding modes of JK-136 (purple), JK-139 (green), and Rhosin (orange) in the RHOA active site. Lipophilic residues of the RHOA cavity are displayed in brown. **b** Superposition of the small molecules, in the RHOA active site. **c** Proposed hydrogen bonding interactions of JK-136 (purple) with the amino acid residues in the active site of RHOA. The key residues are represented in the stick model. The rest of the protein is shown in ribbon cartoon. **d** The proposed hydrogen bonding interaction of JK-139 (green) with the protein residue in the active site of RHOA. The key amino acid residues are represented in the stick model. The rest of the protein is shown in ribbon cartoon.

PLCH2 (phospholipase C2, PLC2), significantly downregulated in JK-136/-139-treated cells, compared with Rhosin treatment (Fig. 5d). Considering that the S1P pathway is activated in cancer cell migration [24], this phenotype is likely downregulated by the two JK compounds through ASAH and PLC, unlike Rhosin.

Animal model confirmation of JK-136 and -139 antitumor effects

For antitumor assessments, nude mice were subcutaneously injected with 1×10^7 MKN-45 or SNU-601 GC cells (mid- and high-RHOA expressing cell lines, respectively) [15], followed by diluted DMSO (vehicle control) or 10 mg/mL Rhosin (2.81×10^4 μM), JK-136 (3.16×10^4 μM), or JK-139 (2.89×10^4 μM), and tumor volumes measured weekly via caliper. After 34 days (completion of the study), growth curves showed superior antitumorigenesis, by JK-136 in MKN-45 (Fig. 6a). In addition, tumors at day 34 showed significant inhibition of RHOA activity by both JK-136 and -139, compared with Rhosin (Fig. 6b). Although Rhosin significantly inhibited RHOA in breast cancer cells [11], we did not detect intratumoral RHOA inhibition in GC xenografts, in contrast to JK-136 (Fig. 6c). Further, we evaluated downstream effects of RHOA, observing significant

A

Compound	Product Structure	k_a ($M^{-1}s^{-1}$)	k_d (s^{-1})	K_D (M)
Rhosin	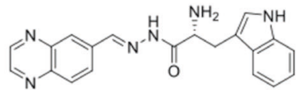	17 ± 1	0.0072 ± 0.0002	420 ± 30μM
JK136	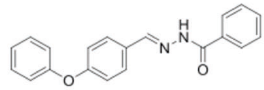	28 ± 1	0.00009 ± 0.00001	3.0 ± 0.1μM
JK139	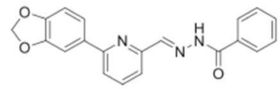	188 ± 8	0.0149 ± 0.0003	79 ± 3μM

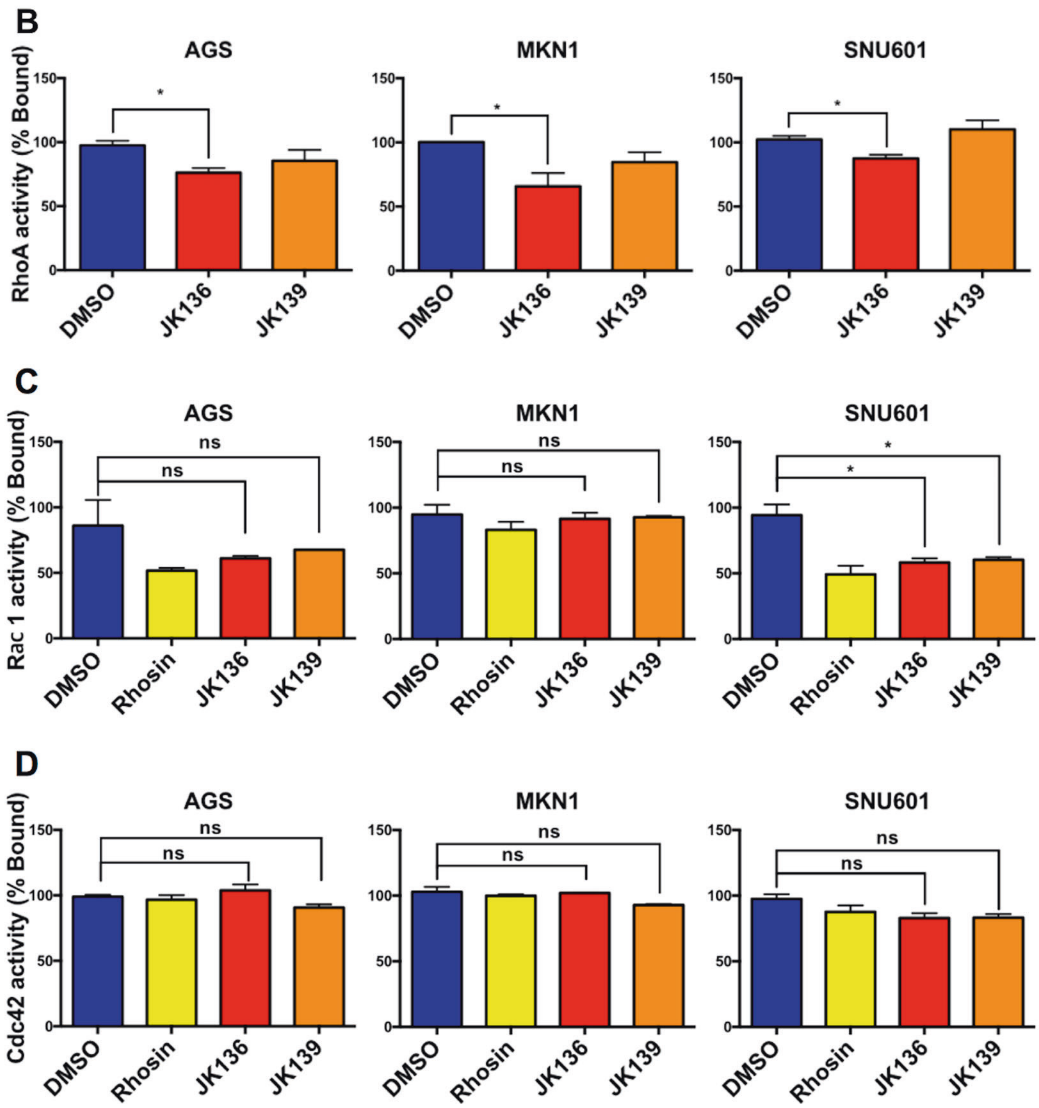

Fig. 4 RHOA inhibitor inhibits activity of RHOA in GC cells. **a** Determination of on and off rates, as well as binding constants (KDs), by surface plasmon resonance. JK-136 showed a significantly higher binding constant than Rhosin. **b** The RHOA activity assay performed in three GC cell lines, JK-136 showed significant inhibition of RHOA activity (*$p < 0.05$). **c**, **d** RAC1 and CDC42 activity assay.

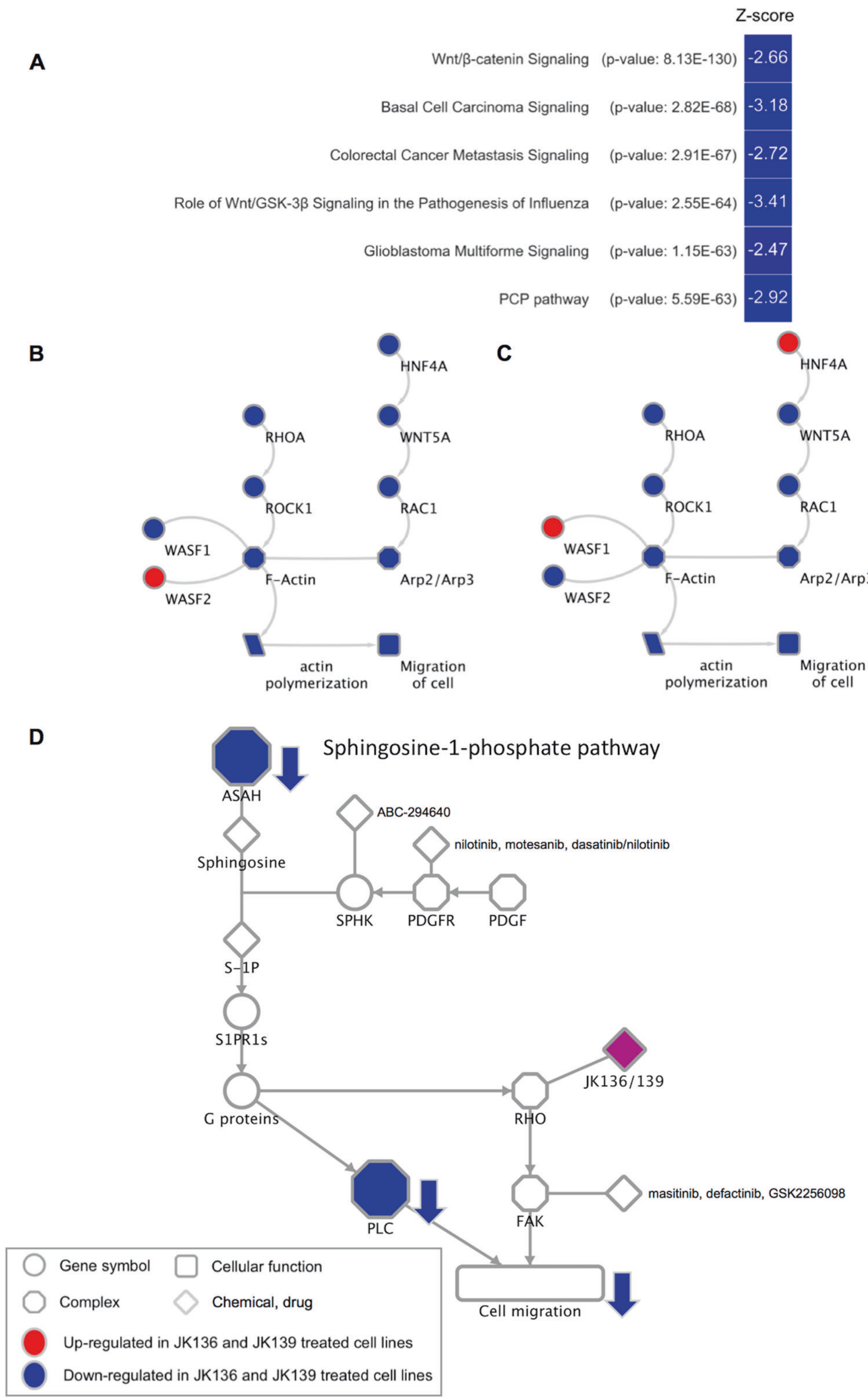

Fig. 5 Network analysis of JK-136 and -139. a IPA analysis of JK-136- and JK-139-treated GC cell lines, showing that canonical Wnt/beta-catenin signaling was downregulated, with an activity *Z*-score of −2.66 (equivalently, inhibition) with gene set enrichment *p* value 8.13E−130. Also, metastasis signaling was downregulated, by each compound. **b** The IPA RHOA signaling network in JK-136- vs. DMSO-treated GC cell lines. Red and blue backgrounds in nodes indicate higher and lower gene expression, respectively, in JK-136- vs. DMSO-treated cell lines. *RHOA*, WAVE complex (*WASF1*), *HNF4A*, and *WNT5A*, as well as *ROCK1*/*RAC1* were downregulated in JK-136-treated cell lines. The IPA-generated original diagram is shown in Supplementary Fig. 3A. **c** IPA RHOA signaling in JK-139- vs. DMSO-treated GC cell lines. Red and blue backgrounds in nodes indicate higher and lower gene expression, respectively, in JK-139- vs. DMSO-treated cell lines. *RHOA*, WAVE complex (*WASF2*), and *WNT5A*, as well as *ROCK1*/*RAC1*, were downregulated in JK-139-treated cell lines. The IPA-generated original diagram is provided in Supplementary Fig. 3B. **d** Difference between JK compounds (JK-136 and -139) and Rhosin in GC cells in sphingosine-1-phosphate signaling. JK compounds downregulated the two genes, *ASAH2B* (indicated in ASAH) and *PLCH2* (indicated in PLC) of the signaling (in comparison with Rhosin treatment), implicating different mode of mechanisms from Rhosin. (S1PRs: S1PR1, S1PR2, S1PR3, S1PR4, and S1PR5. G proteins: Gαi, Gαq, and Gα 12/13).

inhibition of HNF4α protein expression in tumors, by both JK-136 and -139 (Supplementary Fig. S4). This is consistent with our previous study, indicating HNF4α upregulation as a key component of RHOA signaling, in GC tumors [13, 14].

Discussion

Previously, using our subpathway-identification method, PATHOME [13], we identified RHOA activity in GC progression [15], using docking algorithms and SPR to

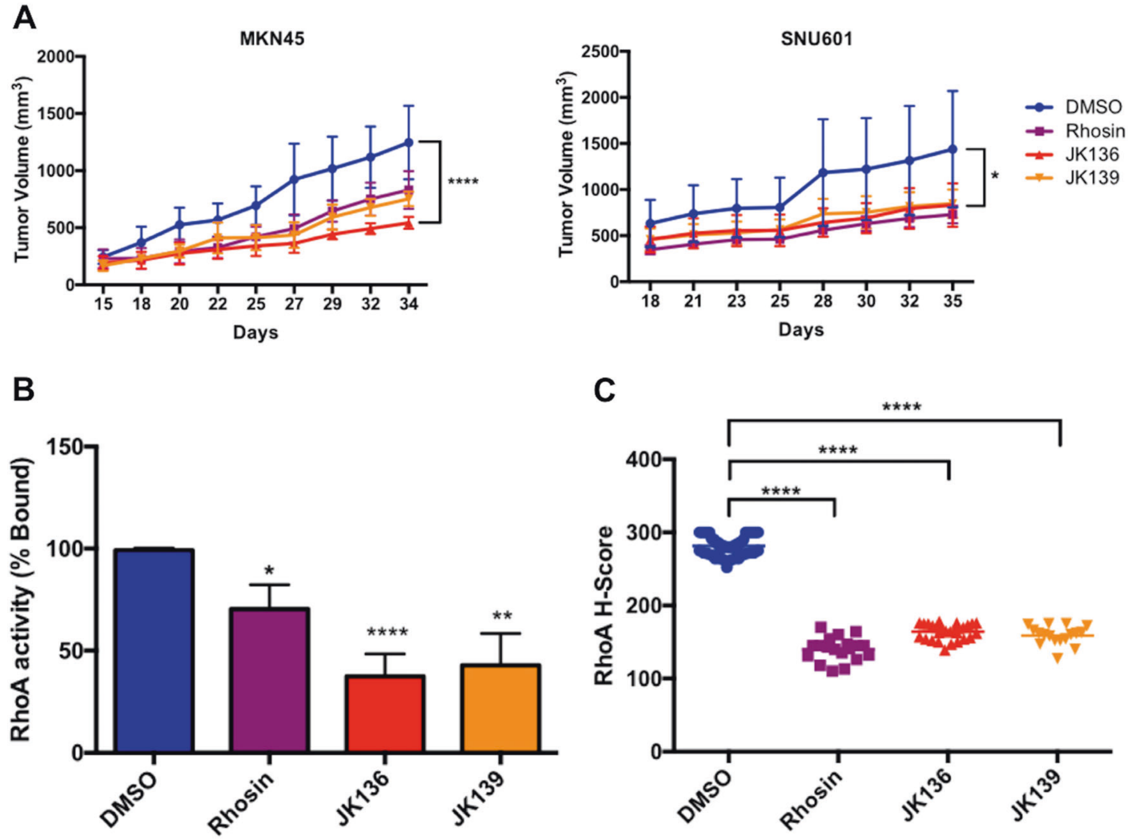

Fig. 6 RHOA inhibitor JK-136 and -139 inhibits tumor activities in animal models. a Antitumor activity of JK-136 and -139 treatment in MKN-45 and SNU-601 GC mouse xenograft models. **b** The RHOA activity assay and **c** immunohistochemistry of xenograft tumors showing significant inhibition of both RHOA activity and RHOA expression levels, by Rhosin, JK-136, and -139 (*$p < 0.05$, **$p < 0.01$, ****$p < 0.001$).

rationally design an active site-binding RHOA inhibitor [15]. Based on that inhibitor, we herein investigated its modifications, based on hydrophobicity and bioactivity. Of these, we obtained two hydrazide analogs, JK-136 and -139, that significantly inhibited GC cell growth, compared with the parent compound and a previously developed, non-clinical RHOA inhibitor, Rhosin [12]. Both JK-136 and -139, compared with Rhosin, more significantly bound immobilized RHOA, and reduced the viability of four GC cell lines of varying RHOA expression, blocked GC cell migration, and significantly impeded tumor growth of mouse GC xenografts.

Other biomarker-based targeted therapeutics have been investigated for GC therapy, with mixed success. For example, trastuzumab (Herceptin®), demonstrated only modest efficacy for HER2-positive GC, in combination with chemotherapy [25]. While targeting of the c-Met and hepatic growth factor oncogenic pathways remains under investigation, epidermal growth factor receptor antagonists have proved unsuccessful for GC [26].

Due to the high degree of heterogeneity in gastric and other cancers, rather than focusing on single pathways, it may be advantageous to target downstream effectors of multiple pathways. For example, targeting RHOA could potentially affect multiple GTPase pathways, in addition to the actin remodeling intrinsically necessary for tumor cell migration/invasion. RHOA inhibition also negatively regulates the cell division control protein CDC42, attenuating the activity of RAC and N-WASP/PAK2, reverting mesenchymal to epithelial morphology, although the specificity of these compounds needs further evaluation [27].

The studies of *Helicobacter Pylori*, the predominant cause of GC, have shown that gastric epithelial host cell phosphorylation of the virulence factor Cytotoxin-Associated Gene A, by the oncogenic tyrosine kinase c-ABL, leads to cell motility [28], and RHOA inhibition blocked cell elongation in infected GC cells [29]. Moreover, Rhosin, significantly reduced numbers of actin stress fibers and focal complexes [12] and herein, we showed our JK-136/-139 compounds to exhibit significantly greater biochemical (RHOA binding) and biological (antitumor) activity than Rhosin. Consequently, impeding determinants of cytoskeletal structure could represent another means of addressing the predicament of oncogenic signaling pathway redundancy.

The studies of other cancer types also suggest RHOA as a possible therapeutic target. For example, intratumoral injection of anti-RHOA siRNA ameliorated growth/angiogenesis of mouse xenografts of highly aggressive and invasive breast cancer cells [30], while another small molecule RHOA inhibitor, CCG-1423, inhibited invasion by PC-3 prostate cancer cells, and induced melanoma cell apoptosis [31]. However, to our knowledge, no RHOA inhibitors have successfully advanced to human cancer clinical trials.

In other GC studies, RHOA has now been linked to cancer stemness and the EMT. For example, shRNA inhibition of the RHOA-activated GTPase, RAC1, reversed drug resistance in MKN-45 GC anchorage-independent cell growth (a hallmark of stemness) [32], and also downregulated the EMT marker Slug [33], while an anti-RHOA shRNA, combined with cisplatin, completely inhibited the growth of MKN-45 and SNU-601 GC xenograft tumors, and expression of the stemness markers CD44 and SOX2 [34]. These studies agree with our in vitro and in vivo studies presented here, for our rationally designed RHOA inhibitors JK-136 and -139.

Recently, the RHOA and WNT signaling pathways have been recognized as therapeutic targets in GC [13–15], although their "crosstalk" was previously unrecognized. In our currently constructed IPA network (Supplementary Fig. S3), WNT5A, previously reported to regulate cell migration, including axon guidance and growth in neurons [35, 36], connected to RAC1, a member of the RHOA signaling network. In fact, in our JK-136 and JK-139-treated GC cell lines, *WNT5A* was downregulated, as well as the WAVE (*WASF1*, *WASF2*) complex. Of interest, JK-136 inhibited gene expression of the HNF4A-WNT5A signaling axis, our previous GC target [14], while JK-139 downregulated only *WNT5A* gene expression, of that axis.

Considering that the RHOA/RAC1/ROCK1/WAVE axis is a common cancer cell migration/invasion-related molecular mechanism, in myriad cancer types [37], our pathway analyses predicted its downregulation by JK-136 and -139, concurring with our cell migration assays. In addition to strong in vitro and in vivo anti-GC efficacy, IPA identified diverse JK-136 and -139-dysregulated pathways, including p53-dependent apoptosis and cell cycle-related pathways.

Previously, we demonstrated that even chemically similar derivatives of small molecules, binding to the same target protein, can elicit different functional contexts [38]. Here, the compounds, JK-136/-139 and Rhosin, binding to RHOA, also showed different functional contexts (Supplementary Table S4). Of interest, an emerging cancer metabolic pathway, S1P, was downregulated by JK-136/-139, in comparison with Rhosin (Fig. 5d). While JK-136 and JK-139 showed better efficacy than Rhosin in in vitro viability assays (Supplementary Table S1), the xenograft models (Fig. 6a) of the two compounds and Rhosin were not correlated to the in vitro assays. This discrepancy between in vitro and in vivo experiments was often observed due to GC heterogeneity [39]. Thus, to find alignment between in vivo and in vitro experiments, further studies based on diverse GC cell line panels and their xenograft models are awaited. Besides therapeutics in cancer, inhibitors should be developed for chemical probes to understand biological mechanisms [40]. Speculating JK-136/-139 as chemical probes, the network analysis of JK-136/-139 treatment in GC cell lines revealed that the S1P signaling pathway was regulated by JK-136 and -139, not by Rhosin. Thus, JK-136/-139 can be chemical probes for RHOA downstreams mediated by the S1P pathway (Fig. 5d).

In summary, we show that pharmacologically optimized hydrazide analogs represent promising targeted, biomarker-driven therapeutics against the tumor- and metastasis-facilitating GTPase oncoprotein RHOA. Through network analysis, we demonstrate highly predictive molecular GC-antineoplastic mechanisms for two such compounds. In mice, these compounds were nontoxic and potently anti-tumorigenic. We assert that in highly heterogeneous tumors, such as GC, computationally predicting and targeting "convergence points" (i.e., "hubs," such as RHOA), of multiple mitogenic pathways, is an emerging strategy for the design of more successful, targeted antineoplastics.

Data availability

GSE135068 in Gene Expression Omnibus.

Acknowledgements This study was supported by grants from the National Research Foundation of Korea (MSIP) (2015R1A2A1A10052661 to YHK), and Basic Science Research Program through the National Research Foundation of Korea (NRF), funded by the Ministry of Education (2016R1D1A1B03933145 to SN). The work was supported by the Gachon University Gil Medical Center (grant number FRD2019–11(2) to SN).

Compliance with ethical standards

Conflict of interest The authors declare that they have no conflict of interest.

References

1. Siegel RL, Miller KD, Jemal A. Cancer statistics, 2017. CA Cancer J Clin. 2017;67:7–30.
2. Luo G, Zhang Y, Guo P, Wang L, Huang Y, Li K. Global patterns and trends in stomach cancer incidence: age, period and birth cohort analysis. Int J Cancer. 2017;141:1333–44.
3. Karimi P, Islami F, Anandasabapathy S, Freedman ND, Kamangar F. Gastric cancer: descriptive epidemiology, risk factors, screening, and prevention. Cancer Epidemiol Biomark Prev. 2014;23:700–13.

4. Jou TS, Nelson WJ. Effects of regulated expression of mutant RhoA and Rac1 small GTPases on the development of epithelial (MDCK) cell polarity. J Cell Biol. 1998;142:85–100.
5. Masiero L, Lapidos KA, Ambudkar I, Kohn EC. Regulation of the RhoA pathway in human endothelial cell spreading on type IV collagen: role of calcium influx. J Cell Sci. 1999;112:3205–13.
6. Gulhati P, Bowen KA, Liu J, Stevens PD, Rychahou PG, Chen M, et al. mTORC1 and mTORC2 regulate EMT, motility, and metastasis of colorectal cancer via RhoA and Rac1 signaling pathways. Cancer Res. 2011;71:3246–56.
7. Nakaya Y, Sukowati EW, Wu Y, Sheng G. RhoA and microtubule dynamics control cell-basement membrane interaction in EMT during gastrulation. Nat Cell Biol. 2008;10:765–75.
8. Coccolini F, Gheza F, Lotti M, Virzi S, Iusco D, Ghermandi C, et al. Peritoneal carcinomatosis. World J Gastroenterol. 2013;19:6979–94.
9. Sun F, Feng M, Guan W. Mechanisms of peritoneal dissemination in gastric cancer. Oncol Lett. 2017;14:6991–8.
10. Kodera Y, Nakanishi H, Ito S, Yamamura Y, Kanemitsu Y, Shimizu Y, et al. Quantitative detection of disseminated free cancer cells in peritoneal washes with real-time reverse transcriptase-polymerase chain reaction: a sensitive predictor of outcome for patients with gastric carcinoma. Ann Surg. 2002;235:499–506.
11. Shang X, Marchioni F, Sipes N, Evelyn CR, Jerabek-Willemsen M, Duhr S, et al. Rational design of small molecule inhibitors targeting RhoA subfamily Rho GTPases. Chem Biol. 2012;19:699–710.
12. Shang X, Marchioni F, Evelyn CR, Sipes N, Zhou X, Seibel W, et al. Small-molecule inhibitors targeting G-protein-coupled Rho guanine nucleotide exchange factors. Proc Natl Acad Sci USA. 2013;110:3155–60.
13. Nam S, Chang HR, Kim KT, Kook MC, Hong D, Kwon CH, et al. PATHOME: an algorithm for accurately detecting differentially expressed subpathways. Oncogene. 2014;33:4941–51.
14. Chang HR, Nam S, Kook MC, Kim KT, Liu X, Yao H, et al. HNF4alpha is a therapeutic target that links AMPK to WNT signalling in early-stage gastric cancer. Gut. 2016;65:19–32.
15. Chang HR, Nam S, Lee J, Kim JH, Jung HR, Park HS, et al. Systematic approach identifies RHOA as a potential biomarker therapeutic target for Asian gastric cancer. Oncotarget. 2016;7:81435–51.
16. Nam S, Kim JH, Lee DH. RHOA in gastric cancer: functional roles and therapeutic potential. Front Genet. 2019;10:438.
17. Cai J, Niu X, Chen Y, Hu Q, Shi G, Wu H, et al. Emodin-induced generation of reactive oxygen species inhibits RhoA activation to sensitize gastric carcinoma cells to anoikis. Neoplasia. 2008;10:41–51.
18. Kansy M, Avdeef A, Fischer H. Advances in screening for membrane permeability: high-resolution PAMPA for medicinal chemists. Drug Disco Today Technol. 2004;1:349–55.
19. Benito DE, Acquaviva A, Castells CB, Gagliardi LG. High throughput method to characterize acid-base properties of insoluble drug candidates in water. J Pharm Biomed Anal. 2018;154:404–12.
20. Jing P, Zhao S, Ruan S, Sui Z, Chen L, Jiang L, et al. Quantitative studies on structure-ORAC relationships of anthocyanins from eggplant and radish using 3D-QSAR. Food Chem. 2014;145:365–71.
21. Katsamba PS, Navratilova I, Calderon-Cacia M, Fan L, Thornton K, Zhu M, et al. Kinetic analysis of a high-affinity antibody/antigen interaction performed by multiple Biacore users. Anal Biochem. 2006;352:208–21.
22. Kramer A, Green J, Pollard J Jr, Tugendreich S. Causal analysis approaches in Ingenuity Pathway Analysis. Bioinformatics. 2014;30:523–30.
23. Chen Z, Borek D, Padrick SB, Gomez TS, Metlagel Z, Ismail AM, et al. Structure and control of the actin regulatory WAVE complex. Nature. 2010;468:533–8.
24. Pyne NJ, Pyne S. Sphingosine 1-phosphate and cancer. Nat Rev Cancer. 2010;10:489–503.
25. Bang YJ, Van Cutsem E, Feyereislova A, Chung HC, Shen L, Sawaki A, et al. Trastuzumab in combination with chemotherapy versus chemotherapy alone for treatment of HER2-positive advanced gastric or gastro-oesophageal junction cancer (ToGA): a phase 3, open-label, randomised controlled trial. Lancet. 2010;376:687–97.
26. Smyth EC, Cunningham D. Targeted therapy for gastric cancer. Curr Treat Options Oncol. 2012;13:377–89.
27. Gadea G, Sanz-Moreno V, Self A, Godi A, Marshall CJ. DOCK10-mediated Cdc42 activation is necessary for amoeboid invasion of melanoma cells. Curr Biol. 2008;18:1456–65.
28. Poppe M, Feller SM, Romer G, Wessler S. Phosphorylation of helicobacter pylori CagA by c-Abl leads to cell motility. Oncogene. 2007;26:3462–72.
29. Lin CJ, Liao WC, Lin HJ, Hsu YM, Lin CL, Chen YA, et al. Statins attenuate helicobacter pylori CagA translocation and reduce incidence of gastric cancer: in vitro and population-based case-control studies. PLoS ONE. 2016;11:e0146432.
30. Pille JY, Denoyelle C, Varet J, Bertrand JR, Soria J, Opolon P, et al. Anti-RhoA and anti-RhoC siRNAs inhibit the proliferation and invasiveness of MDA-MB-231 breast cancer cells in vitro and in vivo. Mol Ther. 2005;11:267–74.
31. Evelyn CR, Wade SM, Wang Q, Wu M, Iniguez-Lluhi JA, Merajver SD, et al. CCG-1423: a small-molecule inhibitor of RhoA transcriptional signaling. Mol Cancer Ther. 2007;6:2249–60.
32. Pastrana E, Silva-Vargas V, Doetsch F. Eyes wide open: a critical review of sphere-formation as an assay for stem cells. Cell Stem Cell. 2011;8:486–98.
33. Yoon C, Cho SJ, Chang KK, Park DJ, Ryeom SW, Yoon SS. Role of Rac1 pathway in epithelial-to-mesenchymal transition and cancer stem-like cell phenotypes in gastric adenocarcinoma. Mol Cancer Res. 2017;15:1106–16.
34. Yoon C, Cho SJ, Aksoy BA, Park DJ, Schultz N, Ryeom SW, et al. Chemotherapy resistance in diffuse-type gastric adenocarcinoma is mediated by RhoA activation in cancer stem-like cells. Clin Cancer Res. 2016;22:971–83.
35. Andersson ER, Prakash N, Cajanek L, Minina E, Bryja V, Bryjova L, et al. Wnt5a regulates ventral midbrain morphogenesis and the development of A9-A10 dopaminergic cells in vivo. PLoS ONE. 2008;3:e3517.
36. Blakely BD, Bye CR, Fernando CV, Horne MK, Macheda ML, Stacker SA, et al. Wnt5a regulates midbrain dopaminergic axon growth and guidance. PLoS ONE. 2011;6:e18373.
37. Yamaguchi H, Condeelis J. Regulation of the actin cytoskeleton in cancer cell migration and invasion. Biochim Biophys Acta. 2007;1773:642–52.
38. Kim JH, Eom HJ, Lim G, Park S, Lee J, Nam S, et al. Differential effects, on oncogenic pathway signalling, by derivatives of the HNF4 alpha inhibitor BI6015. Br J Cancer. 2019;120:488–98.
39. Chang HR, Park HS, Ahn YZ, Nam S, Jung HR, Park S, et al. Improving gastric cancer preclinical studies using diverse in vitro and in vivo model systems. BMC Cancer. 2016;16:200.
40. Castoreno AB, Eggert US. Small molecule probes of cellular pathways and networks. ACS Chem Biol. 2011;6:86–94.